

Thermal Behavior of Alumina Microfibers Precursor Prepared by Surfactant Assisted Microwave Hydrothermal

Xuanmeng He,^{‡,§,†} Guangjun Li,[‡] Hui Liu,[‡] Junqi Li,[‡] and Zhenfeng Zhu[‡]

[‡]School of Materials Science and Engineering, Shaanxi University of Science and Technology, Xi'an 710021, China

[§]Key Laboratory of Auxiliary Chemistry & Technology for Chemical Industry, Ministry of Education, Shaanxi University of Science and Technology, Xi'an 710021, China

Uniform alumina microfibers precursor (ammonium aluminum carbonate hydroxide, AACH) were successfully synthesized using the microwave hydrothermal method, with average length of 5–10 μm and the diameter around 300–500 nm. FT-IR spectra indicated AACH was composed of $\text{NH}_4[\text{Al}(\text{OOH})\text{HCO}_3]\cdot\text{H}_2\text{O}$. The thermal behaviors of the as-prepared AACH were investigated using differential scanning calorimeter and thermogravimetric analysis (DSC-TG), XRD, and SEM. The results showed that the thermal decomposition of the AACH microfibers occurred via three steps, which were respectively divided into adsorption of physical water, dehydration of crystalline water, and decomposition of AACH. The activation energies for the above three steps were calculated using Coats-Redfern method. The phase transformation sequence was found to be $\text{AACH} \rightarrow \text{amorphous Al}_2\text{O}_3 \rightarrow \gamma\text{- and } \theta\text{-Al}_2\text{O}_3 \rightarrow \alpha\text{-Al}_2\text{O}_3$. It was also observed that the thermal treatment had little influence on fiber morphology of the products. The fibers morphology with high thermal stability will endow to prepare alumina microfibers with novel application potentials.

I. Introduction

RECENTLY, one-dimensional (1-D) nanostructure materials, such as nanowires, nanotubes, nanorods, and nanofibers, have attracted considerable interests due to their importance in fundamental research and potential wide-ranging application.^{1,2} One-dimensional alumina nanostructure are highly desirable in areas such as advanced high-temperature composite materials and nanodevices because of their high dielectric constant, good thermal and chemical stability, and high mechanical modulus.^{3,4} Alumina nanostructures could be prepared using various methods, among which the decomposition of ammonium aluminum carbonate hydroxide (AACH) is a promising method to produce alumina. Many efforts have been focused on the preparation of AACH nanostructures, because it can be served as precursor for preparing alumina and inorganic flame-retardants. Bai and co-workers reported the synthesis of alumina microfibers in the presence of AACH as precursors using the copolymer-controlled homogeneous precipitation method under hydrothermal conditions.⁵ Ma *et al.* synthesized net-like AACH particles in a reactor with a mechanical stirrer and a temperature controller under different pH values.⁶ Sun *et al.* described the synthesis of nanometric AACH with a particle

size less than 5 nm using precipitation reaction.⁷ Qin *et al.* reported the preparation of flame-retardant epoxy resins by a mixed method using AACH as a halogen-free flame-retardant.⁸

Kinetic analysis of thermal decomposition processes has been the subject of interest for many investigators all along the modern history of thermal decomposition, because of its importance for designing the device in which the thermal decomposition takes place and analyzing decomposition mechanism.⁹ The Coats-Redfern method for determination of activation energy has been extensively used in kinetic analysis of thermal decomposition process. Sarikaya and co-workers reported the determination of activation energy of an alumina precursor ($\beta\text{-AlOOH}$) for four steps in the thermal decomposition using the Coats-Redfern procedure.¹⁰ Ada *et al.* calculated the activation energy for dehydration and dehydroxylation of the precursor (amorphous alumina) according to Coats-Redfern equation.¹¹

In this study, we presented a simple route to synthesize uniform AACH microfibers with a composition of $\text{NH}_4[\text{Al}(\text{OOH})\text{HCO}_3]\cdot\text{H}_2\text{O}$. The thermal behaviors of AACH microfibers prepared by surfactant-assisted microwave hydrothermal were investigated using differential scanning calorimeter and thermogravimetric analysis (DSC-TG), SEM, and XRD. The activation energy for the steps of AACH in thermal decomposition process were determined using Coats-Redfern equation.

II. Experimental Procedure

(1) Preparations of AACH Microfibers

AACH microfibers were prepared through the hydrothermal reaction of a mixture composed of aluminum sources, surfactant, pH adjusting reagent, and solvents. All chemicals are analytical-grade reagents without further purification. In a typical experiment, 0.4 mmol of polyethylene glycol (PEG)-2000 was dissolved in deionized water to form a clear solution, to which 2.0 mmol of $\text{Al}(\text{NO}_3)_3\cdot 9\text{H}_2\text{O}$ was added. After the alumina salt was totally dissolved, 0.36 mmol of urea was added. The mixed solution was further magnetically stirred for 3 h. Then the solution was transferred into a Teflon-lined autoclave and placed in an oven at 120°C for 24 h. After being cooled to room temperature, the white precipitates were collected and washed several times with deionized water and ethanol to remove the impurities and then dried at 80°C. To study the thermal behavior, calcination was conducted at different temperature in a temperature-programmed muffle furnace.

(2) Characterizations

The crystal structures of as-prepared samples were characterized using X-ray diffraction (XRD-D/max 2200pc, Rigaku,

R. Riman—contributing editor

Manuscript No. 31148. Received April 6, 2012; approved August 15, 2012.

[†]Author to whom correspondence should be addressed. e-mail: hexuanmeng@sust.edu.cn

Tokyo, Japan) technology with $\text{CuK}\alpha$ radiation of wavelength $\lambda = 0.15418$ nm. The microscopic features of samples were characterized using scanning electron microscope (SEM, JSM-6700F; JEOL, Tokyo, Japan) operated at 5 KV, a transmission electron microscope (TEM, JEM2010; JEOL) operated at 200 KV. Thermogravimetric and differential thermal analyses (TGA-DTA) were conducted on a thermogravimetric analyzer (STA449C; Netzsch, Germany), with an air flow rate of 30 mL/min at a heating rate of $10^\circ\text{C}/\text{min}$. Fourier-transform infrared (FT-IR) spectrometer (FT/IR-470; Jasco, Plus, Japan) was used for detection of the AACH precursor and the alumina microfibers.

III. Results and Discussion

The AACH microfibers were prepared using hydrothermal reaction at 120°C for 24 h. The morphologies of as-prepared AACH microfibers are shown in Fig. 1. It can be seen that the sample was made of uniform microfibers. These fibers were not tangled or interwound. The length of fibers is about 5–10 μm , and the diameter is about 300–500 nm. The magnified SEM micrograph [the inset of Fig. 1(B)] shows that the fibers had a very smooth surface, and both ends of each fiber were shrunk to needle-like structure with diameter of about 100 nm. Figure. 1(C) shows the typical XRD pattern of the as-prepared samples, and all of the diffraction peaks can be indexed to crystalline AACH (JCPDS card no. 42-0250). The measured lattice constant “a,” “b,” and “c” of this orthorhombic phase are 6.632, 11.947, and 5.724 Å, which were in good agreement with the theoretical values ($a = 6.618$, $b = 11.944$, and $c = 5.724$ Å, respectively). The high intensities and sharp peaks in Fig. 1(C) indicated that AACH phase synthesized in this work was well crystallized. Using the Scherer equation, the calculated crystallite size of AACH

microfibers is about 6 nm. The high-intensity of (110) crystal face also exhibited that the AACH crystal preferably grew along the given direction under the synthesis condition. No other diffraction peaks were detected, indicating that no impurity exists in as-prepared AACH. Figure 1(D) shows the TEM image of the as-prepared AACH microfibers. The selected area electron diffraction (SEAD) pattern [the inset of Fig. 1(D)] recorded from the face of the crystal having the longest axis (for example, the circled area in TEM image) always exhibited the same single-crystalline pattern, consistent with the [001] zone of AACH crystal. The elongated microfibers shape with the exposed (110) faces demonstrated that the AACH crystal preferably grew along the crystallographic c -axis under the synthesis conditions, which is the same as explanation of XRD dates.

There are two different composition of AACH documented in the literature. Eros and Alrofe¹² found the corrosive products of a piece of aluminum in the atmosphere and identified it as ammonium aluminum hydroxide carbonate with one water ($\text{NH}_4[\text{Al}(\text{OOH})\text{HCO}_3]\cdot\text{H}_2\text{O}$). Kato¹³ synthesized AACH by using the reaction of NH_4HCO_3 and aluminum salt and suggested that the compound had a formula as $\text{NH}_4[\text{Al}(\text{OOH})\text{HCO}_3]$, but the XRD patterns and IR were very close to Erdos and Alrofe’s $\text{NH}_4[\text{Al}(\text{OOH})\text{HCO}_3]\cdot\text{H}_2\text{O}$. Later, Serna, Garcia-Ramos, and Pena¹⁴ also reported the IR results of AACH, which was similar to that reported by Eros and Alrofe’s, but the composition they suggested had no crystal water. From then on, only $\text{NH}_4[\text{Al}(\text{OOH})\text{HCO}_3]$ appeared in almost all of the literature, and no related discussion has been made on the difference of the formula. To clarify the ambiguity of the compound, FT-IR has been done in present study. Figure 2 shows the FT-IR spectra of (a) the as-prepared AACH; (b) AACH dried in a vacuum dryer at 393 K for 24 h, and (c) AACH calcined at

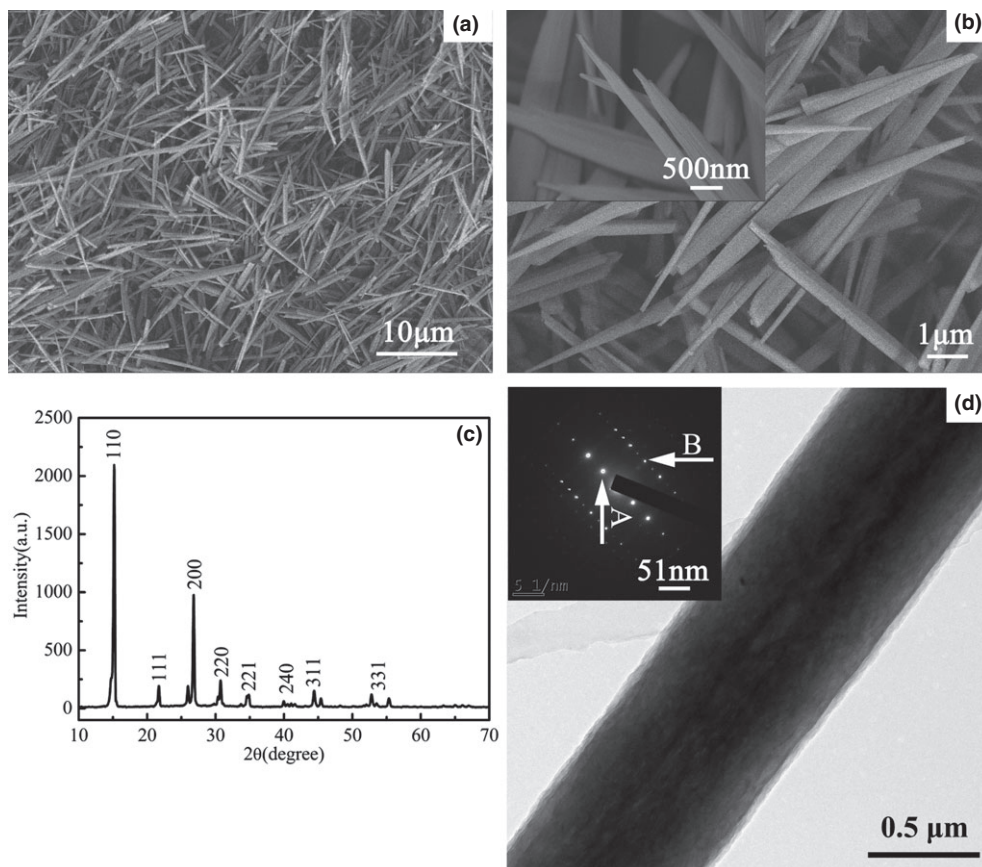


Fig. 1. SEM micrographs of the as-prepared AACH microfibers (a and b), XRD of as-prepared AACH microfibers (c), and TEM image and SEAD pattern of as-prepared AACH microfibers (d).

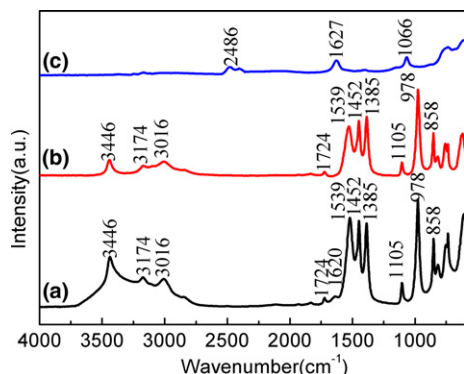


Fig. 2. FT-IR spectra of (a) the as-prepared AACH; (b) AACH dried in a vacuum dryer at 393 K for 24 h; and (c) Al_2O_3 calcined at 773 K for 2 h.

773 K for 2 h. In the spectrum of as-prepared AACH shown in Fig. 2(A), the broad band round 3446 cm^{-1} was attributed to the O-H vibration of adsorbed water.¹⁵ The peaks in the region $3016\text{--}3174\text{ cm}^{-1}$ corresponded to symmetric bending-stretching vibration of NH_4^+ , and around 1385 cm^{-1} was due to asymmetric stretching modes of CO_3^{2-} , the obvious split of this double degenerate peak exhibited that the CO_3^{2-} in the AACH belonged to the structural carbonate group. The weak peak at 1620 cm^{-1} was assigned to the $\delta(\text{H}_2\text{O})$ bending vibration of water molecules adsorbed in the product. The peaks at 1105, 978, and 858 cm^{-1} belonged to C-O-C and $-\text{CH}_2-$ vibration, which originated from the surfactant of PEG. After AACH dried in a vacuum dryer at 393 K for 24 h, the broad peak at 3446 cm^{-1} became weak, and the peak at 1620 cm^{-1} disappeared, indicating gradual decrease of adsorbed water and some water still located between crystals. The FT-IR spectrums of as-prepared AACH and AACH dried in a vacuum dryer at 393 K for 24 h were similar and showed H_2O peak around 3446 cm^{-1} , which indicated that AACH and its dried products have a similar structure, and AACH contained some water which may be located between crystals, identified as a composition of $\text{NH}_4[\text{Al}(\text{OOH})\text{HCO}_3]\cdot\text{H}_2\text{O}$. In the spectrum of AACH calcined at 773 K for 2 h, all absorption peaks of carbonate, ammonium, and organic groups were greatly weakened, even vanishing in the range $1300\text{--}900\text{ cm}^{-1}$, indicating complete decomposition of AACH and formation of Al_2O_3 microfibers.

Thermal properties of the as-prepared AACH were evaluated using TG-DSC. Test conditions were started from 313 to 1573 K at a rate of 10 K/min in a flowing nitrogen environment. The TG-DTG curves of the as-prepared AACH microfibers are shown in Fig. 3. The TG curve shows that the sample has two major weight loss events. The first weight loss below 460 K is due to adsorption of water in the AACH, corresponding to an endothermic peak between 313

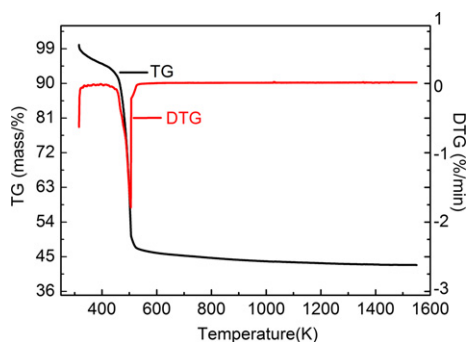


Fig. 3. TG and DTG curves of the as-prepared AACH microfibers.

and 460 K on the DSC curve (Fig. 4). According to the interaction between water and the as-prepared AACH, the dehydration is divided into two steps. The first step is adsorption of physically adsorbed water (a). The second step is that chemical bond between water and AACH is broken, eliminating the crystal water in the AACH (b). The second weight-loss event (c) in the temperature range of 460–530 K, which also can be seen from the aculeated endothermic peak at 510 K of the DSC curve, is associated with the decomposition of PEG-2000, together with the decomposition of AACH, releasing CO_2 , NH_3 , and H_2O and forming AlOOH . The intense endothermic peak indicates that the decomposition of AACH request much energy. Therefore, AACH can be served as a perfect inorganic flame-retardant. With the increasing temperature in the thermal process, the TG curve keeps decreasing in a slight manner, indicating the decomposition of AlOOH and forming the alumina particles. The sole exothermal peak which presents in DSC plot at 1157 K is associated with the phase transition process of the alumina. From the TG curve, it is apparent that the as-prepared AACH contained 58.63% volatile and 41.37% fine alumina powder.

The decrease in mass at each temperature were read from TG curve and their ratios to the total mass loss which remained constant at 800 K was defined as the decomposition fraction (α). The variation of the decomposition fraction as a function of temperature is given in Fig. 5. The inset of Fig. 5 is the magnified variation between 313 and 460 K. In the α - T curve, the section “a” and “b” show, respectively, the first and second dehydrations and section “c” shows the decomposition.

As the mass fraction of decomposition part of the volatile matter in the as-prepared AACH is α , the mass fraction of the part which is not yet decomposed is $(1-\alpha)$. According to Coats-Redfern equation, the chemical reaction kinetics of as-prepared AACH decomposition can be described as follows:

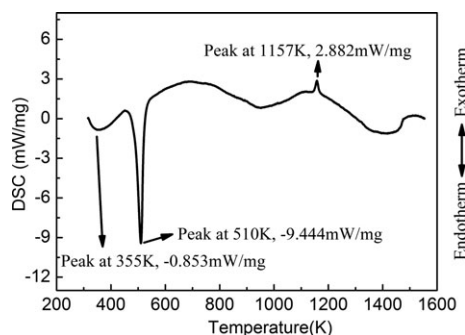


Fig. 4. DSC curve of the as-prepared AACH microfibers.

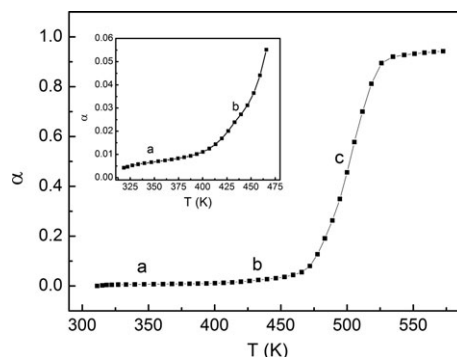


Fig. 5. The variation of decomposition fraction as a function of calcination temperature.

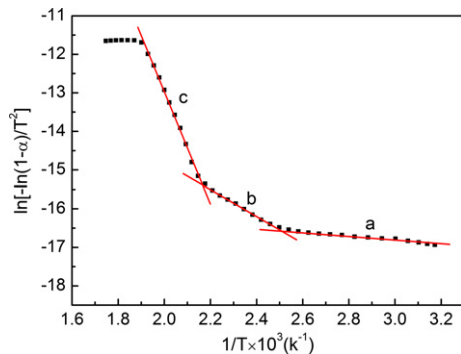


Fig. 6. Fitting the decomposition data to Coats-Redfern equation.

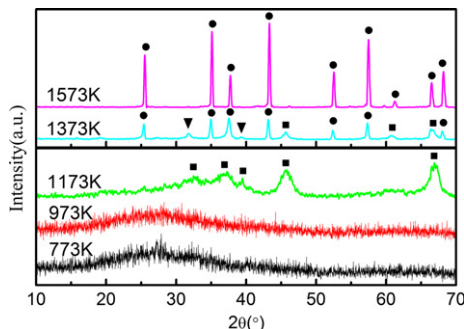


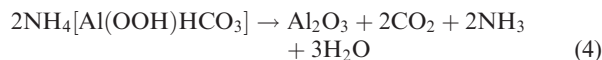
Fig. 7. XRD pattern of the as-prepared samples calcined at different temperatures for 2 h. (●), (■), and (▼) denote the α - Al_2O_3 , γ - Al_2O_3 , and θ - Al_2O_3 .

$$\ln\left\{\frac{-\ln(1-\alpha)}{T^2}\right\} = -E/RT + \ln[(AR/\beta E)(1-2RT/E)] \quad (1)$$

where T is the average deformation temperature, $\beta = dT/dt$ is the heating rate, E is the activation energy of deformation, R is the universal gas constant, and $\ln[(AR/\beta E)(1-2RT/E)]$ is quantity that stays nearly constant. When $\ln[-\ln(1-\alpha)/T^2]$ values calculated using α values at different temperature were plotted as a function of $1/T$, the “a,” “b,” and “c” of straight lines seen in Fig. 6 were obtained. By considering intervals temperature of three straight lines, it is consistent with the section “a,” “b,” and “c” of AACH decomposition. From the slopes of straight line, the activation energies were, respectively, calculated as $E_a = 3.35$ KJ/mol, $E_b = 29.32$ KJ/mol, $E_c = 126.82$ KJ/mol. The fact that E_b was larger than E_a showed that adsorption of physical adsorbed water was a physical event, whereas the dehydration of crystallization water was a chemical event. It was well-known that for the section “c,” where the activation energy was considerably larger than E_b and E_a , $\text{NH}_4[\text{Al}(\text{OOH})\text{HCO}_3]$ is converted to alumina by the release of H_2O , NH_3 , and CO_2 with elevating temperature, as described in the following equation:



Combining the above reactions yields an overall reaction:



To identify the decomposed products of AACH microfibers and the phase transformation of alumina fibers during calcination process, the XRD patterns of calcined products of the as-prepared AACH microfibers were measured. Figure 7 shows the XRD pattern of the as-prepared AACH microfibers calcined at different temperature. After calcinations at 773 and 973 K, both alumina samples essentially became amorphous. By increasing calcination temperature to 1173 K, the γ - and θ - Al_2O_3 phase were observed. The low intensity of XRD peaks indicates that the alumina samples calcined at this temperature has low crystalline, whereas the broad peaks demonstrated that the alumina calcined at 1173 K are nanocrystalline. Further increasing calcination temperature to 1373 K, the α - Al_2O_3 phase is observed. When calcination temperature was increased to 1573 K, a typical XRD pattern of the α - Al_2O_3 phase was obtained. The shape and high intensities of the peaks indicate that the Al_2O_3 is indeed well-crystallized. No other diffraction peaks were detected, indicating that no impurity exists and the AACH microfibers have completely transformed into the α - Al_2O_3 phase.

Figure 8 shows the SEM micrographs of the as-prepared AACH microfibers calcined at 1173 K (A), 1373 K (B), and 1573 K (C), respectively. From SEM investigation, we can see that the morphologies of the alumina microfibers calcined at 1373 and 1573 K, calcinations are similar to those of their counterparts before calcination [Fig. 1(B)]. When calcination temperature was increased to 1573 K, some fibers became curved, possibly because of sintering. However, the essential fiber morphology still remains, which indicate that the heat treatment has little influence on the fiber morphology of the products. The fibers morphology with high thermal stability will endow to prepare alumina microfibers with novel application potentials.

IV. Conclusions

The uniformly sized AACH microfibers have been successfully synthesized using the hydrothermal reaction of a mixture composed of aluminum nitrate, PEG-2000, urea, and solvents. FT-IR spectra indicate AACH with a composition of $\text{NH}_4[\text{Al}(\text{OOH})\text{HCO}_3] \cdot \text{H}_2\text{O}$, different from preceding reports. The thermal decomposition of AACH microfibers occurred via three steps, which was, respectively, divided into adsorption of physical water, dehydration of crystalline water, and decomposition of AACH. All of the three activation energies were calculated using the Coats and Redfern

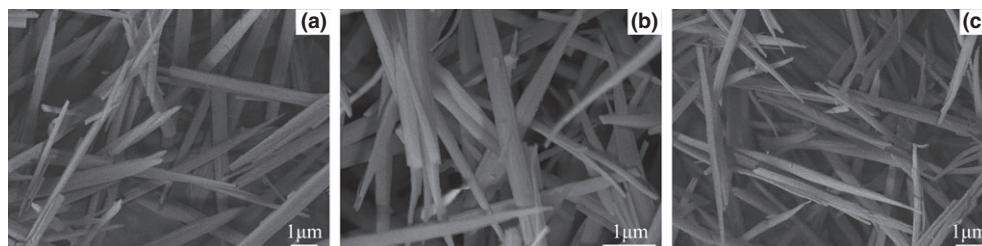


Fig. 8. SEM images of the as-prepared AACH microfibers calcined at 973 K (a), 1173 K (b), and 1373 K (c).

procedure. In the thermal treatment process, AACH was decomposed and formed alumina particles, meanwhile the phase transformations of alumina occurred. The phase transformation sequence was found to be AACH \rightarrow amorphous $\text{Al}_2\text{O}_3 \rightarrow \gamma$ - and θ - $\text{Al}_2\text{O}_3 \rightarrow \alpha$ - Al_2O_3 . Whereas, it was also observed that the thermal treatment had little influence on the fiber morphology of the products. Due to its fiber morphology and high thermal stability, it will endow to prepare alumina microfibers with novel application potentials.

Acknowledgments

This work was financially supported by National Science Foundation of Shaanxi University of Science and Technology (no. zx09-17), China Postdoctoral Science Foundation funded Project (no. 200902584), and the Special Fund from Shaanxi Provincial Department of Education (no. 09JK355).

References

¹Y. Xia, P. Yang, Y. Sun, Y. Wu, B. Mayers, B. Gates, Y. Yin, F. Kim, and H. Yan, "One-Dimensional Nanostructures: Synthesis, Characterization, and Applications," *Adv. Mater.*, **15**, 353–89 (2003).
²X. G. Peng, L. Manna, W. D. Yang, J. Wickham, E. Scher, A. Kadavani, and A. P. Alivisatos, "Shape Control of CdSe Nanocrystals," *Nature*, **404**, 59–61 (2000).
³J. P. Zou, L. Pu, X. M. Bao, and D. Feng, "Branchy Alumina Nanotubes," *Appl. Phys. Lett.*, **80**, 1079–81 (2002).
⁴X. S. Fang, C. H. Ye, L. D. Zhang, and T. Xie, "Twinning-Mediated Growth of Al_2O_3 Nanobelts and Their Enhanced Dielectric Responses," *Adv. Mater.*, **17**, 1661–5 (2005).

⁵P. Bai, F. B. Sun, P. P. Wu, L. K. Wang, F. Y. Lee, L. Lv, Z. F. Yan, and X. S. Zhao, "Copolymer-Controlled Homogeneous Precipitation for the Synthesis of Porous Microfibers of Alumina," *Langmuir*, **23**, 4599–605 (2007).
⁶C. C. Ma, X. X. Zhou, X. Xu, and T. Zhu, "Synthesis and Thermal Decomposition of Ammonium Aluminum Carbonate Hydroxide (AACH)," *Mater. Chem. Phys.*, **72**, 374–9 (2001).
⁷X. D. Sun, J. G. Li, F. Zhang, X. M. Qin, Z. M. Xiu, and H. Q. Ru, "Synthesis of Nanocrystalline α - Al_2O_3 Powders From Nanometric Ammonium Aluminum Carbonate Hydroxide," *J. Am. Ceram. Soc.*, **86** [8] 1321–5 (2003).
⁸L. Q. Qin, L. M. Zhang, Z. X. Huang, Z. J. Huang, and Y. B. Wang, "Synthesis, Characterization and Flame-Retardant Properties of Epoxy Resins and AACHH Composites," *J. Wuhan University of Technology-Mater. Sci. Ed.*, **25** [4] 763–8 (2009).
⁹R. Ebrahimi-Kahrizsangi, and M. H. Abbasi, "Evaluation of Reliability of Coats-Redfern Method for Kinetic Analysis of non-Isothermal TGA," *Trans. Nonferrous Met. Soc. China*, **18**, 217–21 (2008).
¹⁰Y. Sarikaya, I. Sevinc, and M. Akinc, "The Effect of Calcination Temperature on Some of the Adsorptive Properties of Fine Alumina Powders Obtained by Emulsion Evaporation Technique," *Powder Technol.*, **116**, 109–14 (2001).
¹¹K. Ada, Y. Sarikaya, T. Alemdaroglu, and M. Onal, "Thermal Behaviour of Alumina Precursor Obtained by the Aluminium Sulphate-Urea Reaction in Boiling Aqueous Solution," *Ceram. Int.*, **29**, 513–8 (2003).
¹²E. Erdős, and H. Altorfer, "Ein dem Malachit Ähnliches Basisches Eisenkarbonat als Korrosionsprodukt von Stahl," *Mater. Corros.*, **27** [5] 304–12 (1976).
¹³S. Kato, T. Iga, S. Hatano, and Y. Izawa, "Synthesis of $\text{NH}_4\text{AlO}(\text{OH})\text{HCO}_3$," *Yogyo-Kyokai-Shi*, **84** [5] 215–20 (1976).
¹⁴C. J. Serma, J. V. Garcia-Ramos, and M. J. Peña, "Vibrational Study of Dawsonite Type Compounds $\text{MAl}(\text{OH})_2\text{CO}_3$ (M=Na, K, NH_4)," *Spectrochim. Acta, Part A*, **41** [5] 697–702 (1985).
¹⁵K. M. Parida, A. C. Pradhan, J. Das, and N. Sahu, "Synthesis and Characterization of Nano-Sized Porous Gamma-Alumina by Control Precipitation Method," *Mater. Chem. Phys.*, **113**, 244–8 (2009). □